Journal of Advanced Engineering Vol. 8, No. 4, pp. 191-195 / October 2013

基板溫度對 ITO/NPB/Alq3/Al 異質結構之物性的影響
Effects of Substrate Temperature on the Physical Properties of ITO/NPB/Alq3/Al Heterostructures

湯秀靜 蘇志豐 林谷彥 王智祥 邱寬城*
Shiow-Jing Tang, Chih-Feng Su, Ku-Yen Lin, Jyh-Shyang Wang, Kuan-Cheng Chiu*

摘要

本論文利用不同的基板溫度（T_{sub}）於壓力約 10^{-7} Torr 之熱蒸鍍腔體中製作具有 ITO/NPB/Alq3/Al 基本架構之有機發光二極體（OLED）。由原子力顯微鏡、X 光繞射、電流密度與外加偏壓、和發光強度與外加偏壓的特性分析，本文探討所成長之有機分子薄膜及其所製作之 OLED 元件的表面形貌、結構性質、電性與發光特性。當 T_{sub} 由 30℃增加到 90℃，黏著於成長中之介面的有機小分子（NPB 或 Alq3）可獲得較高之表面擴散動能，並導致所成長之有機薄膜具有較平坦的形貌與較緻密的結構。因此，在 T_{sub} = 90℃下所製作之 OLED 具有較高之電致螢光發光效率。

關鍵詞：有機發光二極體，物性量測，基板溫度效應，熱蒸鍍法

Abstract

In this paper, organic light-emitting diodes (OLEDs) with a basic structure of indium tin oxide (ITO)/naphthyl-substituted benzidine derivative (NPB)/tris–8-(hydroxyquinoline) aluminum (Alq3)/Al were fabricated in a thermal evaporation chamber at various substrate temperatures (T_{sub}) under pressure around 10^{-7} Torr. Through atomic force microscopy, x-ray diffraction, current density-voltage and luminescence intensity-voltage analysis, a study on surface morphology, structural information, electrical and optical properties of the as-deposited organic layers as well as the as-fabricated OLEDs was performed. With increasing T_{sub} from 30℃ to 90℃, the adhering organic molecules on the growing interface gain more surface diffusion energy, and the as-deposited organic layers possess flatter surface morphology and more compact structure. Accordingly, higher values of electroluminescence efficiency were obtained from OLEDs fabricated at T_{sub} = 90℃.

Keywords: organic light-emitting diodes, physical characterization, effect of substrate temperature, thermal evaporation chamber

I. INTRODUCTION

Over the past two decades, a tremendous progress has been achieved in the field of organic light-emitting diodes (OLEDs) due to an intensive research effort on the preparation and characterization of the organic semiconducting thin films and on the optimization of the device structures [1-15]. The active layers in these devices are fabricated from small organic molecules, oligomers and/or polymers. These molecular solids formed by weak van der Waals force have in common a conjugated π-electron system within which electrons can move via the overlap of π-electron clouds. The performance of OLEDs including the luminous intensity, lifetime and stability is sensitively determined by injection of charge carriers through the metal/organic interfaces, transport of charge carriers across the organic molecular layers, and recombination of electron-hole pairs near the organic/organic interface. All these transport properties and recombination efficiency are profoundly dependent on the packing of these organic molecules and hence are closely related to the deposition processes.

Organic layers from small molecules or conjugated oligomers can be prepared by thermal evaporation on a cold substrate [1, 11-13] or a heated substrate [14, 15]. The layers deposited on a cold substrate without heating are usually not macroscopically homogeneous because of the low thermal diffusion energy of the adhered small organic

中原大學物理學系與奈米科技中心
*Corresponding author. E-mail: kcchiu@cycu.edu.tw
Department of Physics and Center for Nanotechnology, Chung Yuan Christian University, Chung-Li, Taiwan, R.O.C.
Manuscript received 16 May 2013; revised 10 July 2013; accepted 17 July 2013

molecules. The effects of substrate temperature T_{sub} and source temperature T_{sou} on the physical properties of tris-8-(hydroxyquinoline)aluminum (Alq3) amorphous layers had been clearly observed [16-18]. To extend these experimental findings from a single layer structure to a complicated and sophisticated optoelectronic heterostructure, a systematic study of the effects of deposition conditions on the physical properties of as-fabricated OLEDs was performed. In this work, naphthyl-substituted benzidine derivative (NPB) was used as a hole transport layer, Alq3 as an electron transport and luminescent layer, and indium tin oxide (ITO)-coated glass as a substrate. A simple structure of ITO/NPB/Alq3/Al was adopted, which was one of the remarkable and important heterostructures used in OLEDs [1-15]. Because the glass-phase transition temperature (T_g) of NPB is around 85℃, to further investigate the effects of T_{sub} on NPB layer (below and above its T_g) as well as on ITO/NPB/Alq3/Al heterostructure, the samples were fabricated in a thermal evaporation chamber at T_{sub} = 30℃ and 90℃, respectively. The physical properties (including surface morphology and structural information) of these as-deposited organic thin films (in layer-by-layer sequence) were measured by atomic force microscopy (AFM) and x-ray diffraction (XRD). In addition, by measuring the current density-luminescence intensity-bias voltage (*J-L-V*) characteristics, the performance of these as-fabricated OLEDs was discussed with respect to T_{sub}.

II. EXPERIMENTAL PROCEDURES

The samples were prepared in a thermal evaporation chamber with a based pressure of about 3×10^{-7} Torr. ITO conducting glass with sheet resistance of 13 ± 2 Ω/square and with thickness of 150 ± 25 nm was used as a substrate. The distance between source crucible and ITO substrate was about 42 cm. The value of T_{sou} was fixed around 170 to 200℃ for NPB and around 250 to 300℃ for Alq3, respectively, and the values of T_{sub} were varied from 30℃ to 90℃. Commercially available source powders NPB (with purity of 99.0%, sublimed) and Alq3 (sublimed) were used as received and were loaded separately in boron nitride crucibles. After the pressure of the chamber reached about 3×10^{-7} Torr, the heating system started. For ITO-substrate, T_{sub} was first slowly increased up to 300℃ to thermally clean the interface and to activate the surface activity, and then cooled off naturally to the setting value. For source powder, an *in situ* cleaning process was applied, *i.e.*, before heating directly to the setting value of T_{sou}, the crucible was stayed at about 75℃ for 20 min and 125℃ for 10 min for additional heat treatment in order to evaporate any possible moisture or impurities involved during the handling of source powder into the system. When T_{sou} and T_{sub} attained the setting values, the shutter in between the source crucibles and substrate was removed to allow thermal evaporation of the source molecules onto the substrate. The deposition rate was maintained at 4-6 Å/s for NPB and 2-3 Å/s for Alq3, respectively. After the thickness of NPB film reached the required value, the heating system was turned off and cooled down naturally. Then, the deposition process repeated again for Alq3 thin film. To focus on the T_{sub}-effect on the properties of the organic layers, the thickness of the as-deposited NPB and Alq3 layers was kept around 100 nm (slightly larger than that in typical OLEDs) to achieve a better uniformity. Finally, the vacuum was broken and a mask was inserted in front of the sample; and Al thin-film with an active area of 0.15 cm^2 and a thickness of 100 nm was thermally evaporated again on top of ITO/NPB/Alq3 in vacuum as the cathode.

For sample characterization, AFM image was obtained by a scanning force microscope (NT-MDT Solver P47) in tapping mode. XRD measurement was carried out on an X-ray diffractometer (PANalytical PW 3040/60 X'Pert Pro) with Cu-Kα emission. *J-V* characteristic was measured by an electrometer (Keithley 2400) in *I-V* mode and electroluminescence (EL) intensity was recorded by an optometer (Newport 1830C) located about 3 cm away from the OLED at room temperature.

III. RESULTS AND DISCUSSION

Fig. 1 presents the typical AFM pictures of the surface morphology of ITO glass as received and post-annealed at 300℃ for 1 h in vacuum. From our previous work, we found that the annealing temperature up to 300℃ for 1 h does not change the sheet resistance of ITO very much (within 8% only). However, the 300℃-annealing process does lead the surface atoms to aggregate and to form larger grains, and the calculated root-mean-square roughness R_{rms} of the ITO surface decreases from 2.05 ± 0.10 nm to 1.47 ± 0.11 nm. Similar effect was reported for the post-annealed ITO substrate in air at 250℃ for 1 h [19]. From XRD patterns as depicted by Fig. 2, the as-received ITO glass exhibits two clear and

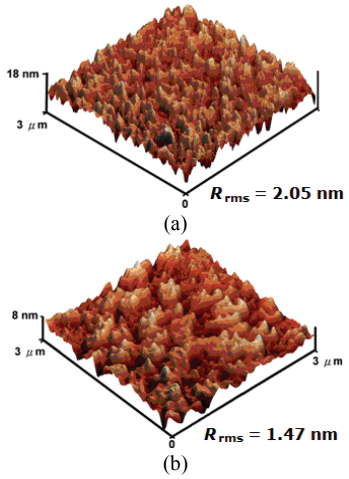

Fig. 1 AFM pictures for ITO substrates (a) as received and (b) post-annealed at 300℃ for 1 h in vacuum

distinguishable peaks at 30.6° and 35.5° which correspond to (222) and (400) planes, respectively [19]. In addition, a broad diffuse peak (due to an amorphous character) representing an average nearest-neighbor distance is superimposed. As the ITO substrate being annealed, the shape of this broad diffuse peak shifts to a slightly asymmetric distribution as shown in Fig. 2(b). Due to the improvements of surface morphology and crystallinity as abovementioned, all ITO substrates used in the following sample preparation were post-annealed *in situ* within the vacuum chamber in order to increase the adhesion of the incoming organic molecules on the ITO surface.

During thermal evaporation in a vacuum chamber, T_{sou} determines the vapor pressure of source powder and plays an important role in determining the growth rate of the as-deposited film [17, 18]. However, if T_{sou} is too high, the organic source compounds tend to decompose easily. Therefore, $T_{sou} \fallingdotseq$ 170 to 200℃ for NPB and 250 to 300 ℃ for Alq3 were usually adopted to have a better control of the quality and thickness of the as-deposited films.

Figs. 3 and 4 present the AFM and XRD patterns for ITO/NPB and ITO/NPB/Alq3 heterostructures with respect to T_{sub} = 30℃ and 90℃. As depicted in Fig. 3, on top of the post-annealed ITO interface (with R_{rms} = 1.47 ± 0.11 nm) and at T_{sub} = 30℃, after the deposition of a thin amorphous layer of NPB with thickness of 100 nm (ITO/NPB), R_{rms} increases from 1.47 nm (ITO) up to 1.87 ± 0.03 nm; and after the deposition of an additional Alq3 layer with thickness 100 nm (ITO/NPB/Alq3), R_{rms} decreases down to 1.50 ± 0.10 nm. However, at T_{sub} = 90 ℃, R_{rms} decreases from 1.47 nm (ITO) to 1.06 ± 0.08 nm (ITO/NPB), and again down to 0.80 ± 0.05 nm (ITO/NPB/Alq3). Furthermore, from the XRD patterns as illustrated in Fig. 4, with T_{sub} = 30℃, after the deposition of a thin amorphous NPB layer and an additional thin amorphous Alq3 layer (both of 100 nm), the XRD peaks as shown in Figs. 4(a) and 4(b) remain the same which indeed are characteristics from the underneath ITO substrate [19]. However, at T_{sub} = 90℃, the intensity of these four ITO-related peaks reduces slightly as shown in

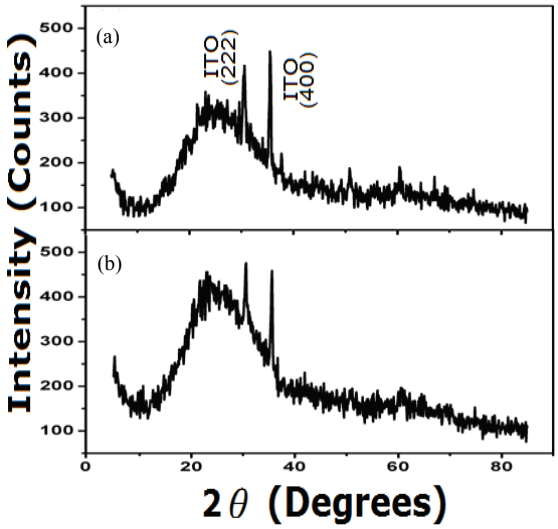

Fig. 2 XRD patterns for ITO substrates (a) as received and (b) post-annealed at 300℃ for 1 h in vacuum

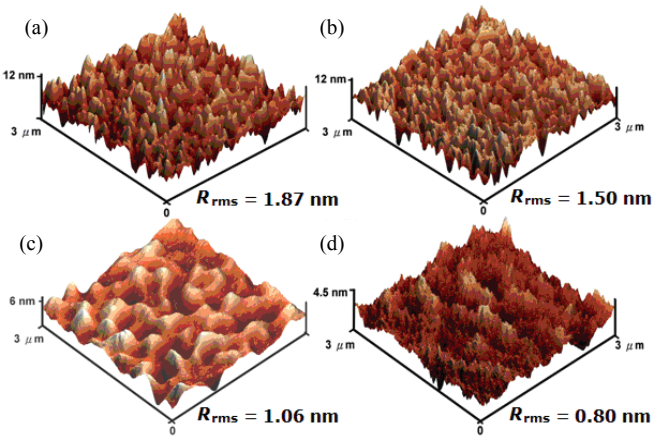

Fig. 3 Surface morphology for (a) ITO/NPB and (b) ITO/NPB/Alq3 heterostructures deposited at T_{sub} = 30℃; and (c) ITO/NPB and (d) ITO/NPB/Alq3 heterostructures deposited at T_{sub} = 90℃

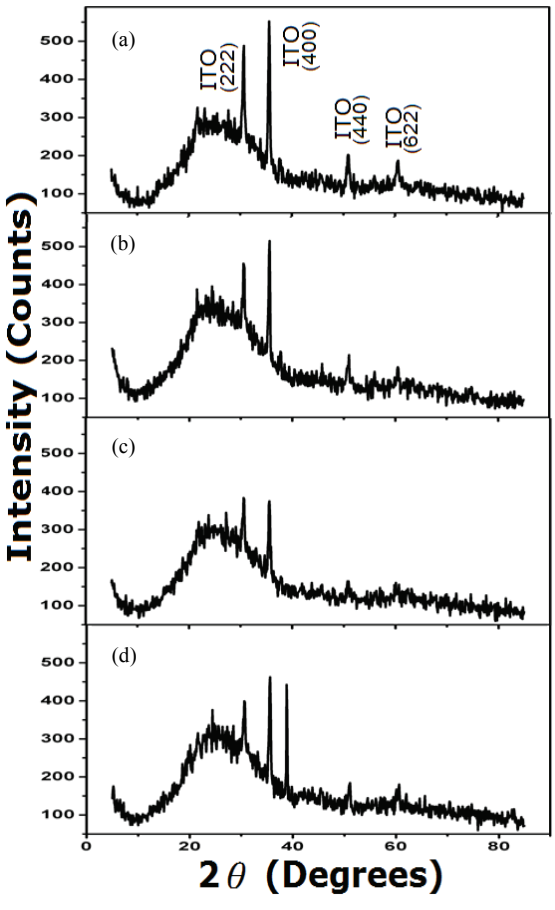

Fig. 4 XRD patterns for (a) ITO/NPB and (b) ITO/NPB/Alq3 heterostructures deposited at T_{sub} = 30℃; and (c) ITO/NPB and (d) ITO/NPB/Alq3 heterostructures deposited at T_{sub} = 90℃

Fig. 4(c), and an additional peak at $2\theta = 38.8°$ appears as depicted in Fig. 4(d). This peak could be attributed to a complex interaction of the adhered Alq3 molecules and the NPB grains at a higher T_{sub} of 90℃. Because T_g of NPB is around 85℃, the deposition of NPB and Alq3 layers at 90 ℃ (see also the granular-like structures as illustrated in Figs. 3(c) and 3(d)) may result in a formation of some tiny crystalline grains. To understand the formation mechanism of this crystalline phase, a further study is undertaken by this group. Above AFM and XRD results reveal that with T_{sub} slightly increasing from 30℃ up to 90℃ the adhered small organic (NPB or Alq3) molecules on the growing interface gain more surface diffusion energy. Thus, the as-deposited layer (formed by a rather weak van der Waals force) then possesses flatter surface morphology and more compact structure; and the subsequent deposition of Alq3 thin film not only tends to smooth the roughness of the underneath NPB interface, but could also results in a complex interaction to form a new crystalline grain at a higher T_{sub} of 90℃.

Fig. 5 gives the *J-V* (with open squares) and *L-V* (with open circles) characteristics of ITO/NPB(100 nm)/Alq3(100 nm)/Al OLEDs fabricated at T_{sub} = 30℃ and 90℃, respectively. From the lowest detection limit of our optical power meter, the threshold voltage V_T for luminescence is defined as the EL intensity exceeds 2×10^{-5} mW/cm^2 (which has been converted into the intensity on the planar surface of OLEDs). For our samples as shown in the insets of Fig. 5, the values of V_T are 19.4 V (for T_{sub} = 30℃) and 21.6 V (for T_{sub} = 90℃). These higher values of V_T obtained in this work were due to the larger layer-thickness deposited (a total of 200 nm as compared to the typical film-thickness of about 135 nm or less [1, 11-15]) and the vacuum break for mask alignment before the deposition of Al-electrode in these as-fabricated OLEDs.

By comparing the ratio of the output EL intensity versus the input electric power density $J\times V$, the relative EL efficiency is defined by $\eta = L/(J\times V)$ for $V > V_T$. As shown in Fig. 6, the values of η for OLEDs fabricated at T_{sub} = 90 ℃ are about a factor of three larger than those values for OLEDs fabricated at T_{sub} = 30℃. In addition, it is reported that the partially crystalline NPB layer should possess less degradation problems for the subsequent operation and storage of the as-fabricated OLEDs [14]. This present investigation further illustrated that a relatively higher value of η for OLED fabricated at a higher T_{sub} of 90℃ can be obtained as compared to that prepared on a cold substrate without external heating.

Above experimental results suggest that the deposition conditions, especially for T_{sub}, profoundly affect the physical properties of organic molecular solids as well as the performance of the as-fabricated OLEDs. Therefore, a consideration to include the effects of T_{sub}-dependence in fabrication processes will be very useful in the design and development for future organic opto-electronic devices.

IV. SUMMARY

OLEDs with a basic structure of ITO/NPB/Alq3/Al were fabricated in a thermal evaporation chamber at T_{sub} = 30℃ and 90℃, respectively. A study on surface morphology, structural information, electrical and optical properties of the as-deposited organic layers as well as the

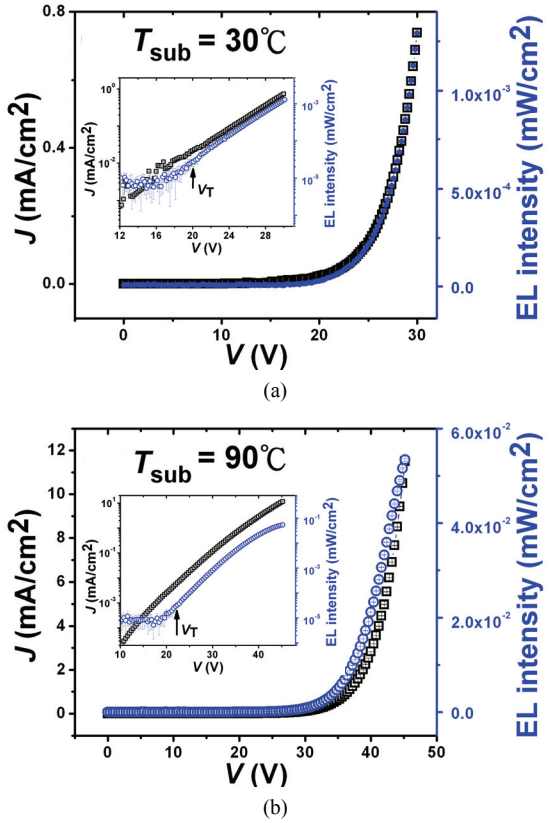

Fig. 5 *J-V* (with open squares) and *L-V* (with open circles) characteristics of the ITO/NPB(100 nm)/Alq3(100 nm)/Al OLEDs fabricated at T_{sub} = (a) 30℃ and (b) 90℃

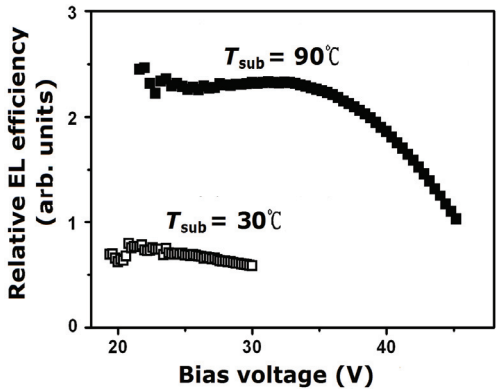

Fig. 6 The values of relative EL efficiency versus bias voltage *V* for the ITO/NPB(100 nm)/Alq3(100 nm)/Al OLEDs fabricated at T_{sub} = (a) 30℃ and (b) 90℃

as-fabricated OLEDs was performed. This work demonstrates that, during the growth processes for OLEDs, with T_{sub} slightly increasing from 30℃ to 90℃ (above T_g of NPB), the adhering organic molecules on the growing interface gain more surface diffusion energy, and the as-deposited layer possesses flatter surface morphology and more compact structure. Accordingly, relatively higher values of η were obtained for OLEDs fabricated at T_{sub} = 90℃.

ACKNOWLEDGMENT

The authors thank the National Science Council of the Republic of China for supporting this research.

REFERENCES

[1] C. W. Tang and S. A. Vanslyke, "Organic electroluminescent diodes," *Appl. Phys. Lett.*, vol. 51, pp. 913-915, 1987.
[2] J. H. Burroughes, D. D. C. Bradley, A. R. Brown, R. N. Marks, K. Mackay, R. H. Friend, P. L. Burns, and A. B. Holmes, "Light-emitting diodes based on conjugated polymers," *Nature*, vol. 347, pp. 539-541, 1990.
[3] Z. H. Kafafi, *Organic Electroluminescence*, Boca Raton: Taylor & Francis, 2005.
[4] W. Brutting, *Physics of Organic Semiconductors*, Weinheim: Wiley-VCH, 2005.
[5] K. Mullen and U. Scherf, *Organic Light Emitting Devices, Synthese, Properties and Applications*, Weinheim: Wiley-VCH, 2006.
[6] S. Miyata and H. S. Nalwa, *Organic Electroluminescent Materials and Devices*, Amsterdam: Gordon and Breach Pub., 1997.
[7] L. S. Hung and C. H. Chen, "Recent progress of molecular organic electroluminescent material and devices," *Mater. Sci. Eng. R.*, vol. 39, pp. 143-222, 2002.
[8] S. H. Hwang, C. N. Moorefield, and G. R. Newkome, "Dendritic macromolecules for organic light-emitting diodes," *Chem. Soc. Rev.*, vol. 37, pp. 2543-2557, 2008.
[9] N. R. Armstrong, W. Wang, D. M. Alloway, D. Placencia, E. Ratcliff, and M. Brumbach, "Organic/organic' heterojunctions: organic light emitting diodes and organic photovoltaic devices," *Macromol. Rapid Commun.*, vol. 30, pp. 717-731, 2009.
[10] A. Chaskar, H. F. Chen, and K. T. Wong, "Bipolar host materials: a chemical approach for highly efficient electrophosphorescent devices," *Adv. Mater.*, vol. 23, pp. 3876-3895, 2011.
[11] K. Hong and J. L. Lee, "Recent developments in light extraction technologies of organic light emitting diodes," *Electro. Mater. Lett.*, vol. 7, pp. 77-91, 2011.
[12] S. A. Van Slyke, C. H. Chen, and C. W. Tang, "Organic electroluminescent devices with improved stability," *Appl. Phys. Lett.*, vol. 69, pp. 2160-2162, 1996.
[13] E. W. Forsythe, D. C. Morton, C. W. Tang, and Y. Gao, "Trap states of tris-8-(hydroxyquinoline) aluminum and naphthyl -substituted benzidine derivative using thermally stimulated luminescence," *Appl. Phys. Lett.*, vol. 73, pp. 1457-1459, 1998.
[14] S. T. Lee, C. S. Lee, Z. Q. Gao, B. J. Chen, W. Y. Lai, and T. C. Wong, "Performance optimization of organic electroluminescent devices," *SPIE Conf. Proc.*, vol. 3797, pp. 138-156, 1999.
[15] D. S. Qin, D. C. Li, Y. Wang, J. D. Zhang, Z. Y. Xie, G. Wang, L. X. Wang, and D. H. Yan, "Effects of the morphologies and structures of light-emitting layers on the performance of organic electroluminescent devices," *Appl. Phys. Lett.*, vol. 78, pp. 437-439, 2001.
[16] A. B. Djurišić, C. Y. Kwong, W. L. Guo, T. W. Lau, E. H. Li, Z. T. Liu, H. S. Kwok, L. S. M. Lam, and W. K. Chan, "Spectroscopic ellipsometry of the optical functions of tris (8-hydroxyquinoline) aluminum (Alq3)," *Thin Solid Films*, vol. 416, pp. 233-241, 2002.
[17] J. M. Chung, Y. Z. Luo, Z. A. Jian, M. C. Kuo, C. S. Yang, W. C. Chou, and K. C. Chiu, "Effects of substrate temperature on the properties of Alq3 amorphous layers prepared by vacuum deposition," *Jpn. J. Appl. Phys.*, vol. 43, pp. 1631-1632, 2004.
[18] Z. A. Jian, Y. Z. Luo, J. M. Chung, S. J. Tang, M. C. Kuo, J. L. Shen, K. C. Chiu, C. S. Yang, W. C. Chou, C. F. Dai, and J. M. Yeh, "Effects of isomeric transformation on characteristics of Alq3 amorphous layers prepared by vacuum deposition at various substrate temperatures," *J. Appl. Phys.*, vol. 101, pp. 123708-123713, 2007.
[19] T. Sasabayashi, N. Ito, E. Nishimura, M. Kon, P. K. Song, K. Utsumi, A. Kaijo, and Y. Shigesato, "Comparative study on structure and internal stress in tin-doped indiumnc oxide films deposited by r.f. magnetron sputtering," *Thin Solid Films*, vol. 445, pp. 219-223, 2003.